

---

# Localized Curvature-based Combinatorial Subgraph Sampling for Large-scale Graphs

---

Anonymous Author(s)

Affiliation

Address

email

## Abstract

1 This paper introduces a subgraph sampling method based on curvature to train  
2 large-scale graphs via mini-batch training. Owing to the difficulty in sampling glob-  
3 ally optimal subgraphs from large graphs, we sample the subgraphs to minimize the  
4 distributional metric with combinatorial sampling. In particular, we define a com-  
5 binatorial metric that distributionally measures the similarity between an original  
6 graph and all possible node and edge combinations of the subgraphs. Further, we  
7 prove that the subgraphs sampled using the probability model proportional to the  
8 discrete Ricci curvature (*i.e.*, Ollivier-Ricci curvatures) of the edges can minimize  
9 the proposed metric. Moreover, as accurate calculation of the curvature on a large  
10 graph is challenging, we propose to use a localized curvature considering only  
11 3-cycles on the graph, suggesting that this is a sufficiently approximated curvature  
12 on a sparse graph. In addition, we show that the probability models of conventional  
13 sampling methods are related to coarsely approximated curvatures with no cycles,  
14 implying that the curvature is closely related to subgraph sampling. The experi-  
15 mental results confirm the feasibility of integrating the proposed curvature-based  
16 sampling method into existing graph neural networks to improve performance.

## 17 1 Introduction

18 Most graph data that represent real-world information tend to be on a large scale, with many nodes  
19 and edges. However, the training of such large-scale graphs with finite computational resources is  
20 challenging, owing to the rapid increase in complexity because of the expanding neighbors. Thus, a  
21 large graph must be transformed into smaller subgraphs to facilitate the use of various graph neural  
22 models, regardless of the size of the graph. However, inevitable errors are induced by unsampled  
23 nodes and edges when the original large-scale graph is divided into independent subgraphs. In general,  
24 graph neural models aggregate neighbor node features along with graph structures. Because subgraphs  
25 are composed of partial nodes and edges, they have sparse structures that aggregate only a portion of  
26 the adjacent nodes.

27 In this paper, we argue that informative subgraphs can be made similar to the original graph using  
28 only partial nodes and edges. Consequently, we present a distributional metric that measures the  
29 accuracy of a subgraph when approximating the distribution defined in the original graph. In addition,  
30 we present a combinatorial distributional metric that measures the similarity (as an expected value)  
31 between all the subgraphs sampled from the probability model and the original graph. This allows us  
32 to recognize distributional differences using only sampling probability models, thus eliminating the  
33 need for actual subgraph samples.

34 We find that sampling the edges with large curvatures is equivalent to reducing the proposed distribu-  
35 tional difference. Curvature is a geometric property that represents the local structure of a space. In  
36 particular, the discrete Ricci curvature (Ollivier-Ricci curvature) can be defined in the graph structure.  
37 Thus, many studies have suggested that the structural information of graphs can be employed via  
38 the curvature. In context of these studies, we suggest that curvature can also be utilized for subgraph  
39 sampling in the course of mini-batch training of large graphs. Consequently, through suitable experi-  
40 ments, we demonstrate that the proposed **Localized Curvature(LoCur)**-based subgraph sampling  
41 method improves the performance of various graphs and graph neural models.

## 42 2 Related Work

43 Graph neural networks (GNNs) have been proposed for learning useful information from graph  
44 data. However, in the process of aggregating connected adjacent nodes, computational costs tend to  
45 increase rapidly with increase in the size of the graph. Thus, the following approaches are introduced  
46 to efficiently learn large-scale graphs.

47 **(Parameters Saving)** The first approach involves reducing parameters of GNNs. In general, the  
48 accuracy of GNNs is not linearly proportional to the size of parameters. Thus, in [39], the linear  
49 activated swallow GNN learned the feature space that approximates deep non-linear activated GNNs.  
50 In [11], the parameters of the GNN model were parallelized. However, because these methods are  
51 based on specific models, they cannot be easily combined with various GNNs.

52 **(Computation Saving)** The second approach involves dynamic selection of the nodes to be con-  
53 sidered for each layer. To realize this, the neighbor sampling method with historical activation was  
54 proposed [4], and the variance was reduced via neighbor sampling-based training. Further, the iid  
55 node importance sampling by Monte-Carlo approach was proposed to prevent recursive neighbor-  
56 hood expansion [5]. These methods approximated the mini-batch gradients. In [17], the conditional  
57 probability model for each layer was learned, and the nodes computed in the next layer were sampled  
58 according to the probabilities. However, these methods are not model-free methods.

59 **(Input Saving)** The third approach involves sampling relatively small subgraphs as inputs to train  
60 networks. The subgraph sampling methods include graph coarsening, graph partitioning, and graph  
61 covering. For example, graphs were filtered through spectral coarsening [33, 9], and adaptive edge  
62 masks were used to drop connections [15]. However, these methods sampled the edges to render  
63 sparse graphs [43], wherein the number of nodes were not reduced but only edges were removed. In  
64 [18, 3], linked nodes were merged into a hyper node to reduce the size of the subgraph. However, this  
65 method encountered difficulties in solving node classification problems, which needs to classify each  
66 node. In contrast, the following method obtained a subgraph using only structure information without  
67 node features. These methods are applicable to large graphs because they sample the subgraphs  
68 via combinatorial node and edge samplings. In [14], a subgraph was obtained by sampling the  
69 neighborhoods of the seed nodes. In [45], subgraph sampling methods were proposed based on node  
70 degrees, edge weights, and random walks. In [7], a subset of clusters was used as a subgraph through  
71 graph clustering. In [1], personalized page rank scores were used to sample nodes in a subgraph.

72 **(Curvature on Graphs)** The graph-structured data is a dependent object, in which nodes are  
73 connected along edges. In addition, the curvature is defined based on structural information. The  
74 Ollivier-Ricci curvature was proposed in [28] considering random-walk-based probability measures  
75 with the Markov chain and the 1-Wasserstein transportation distance to compute the distance between  
76 the probability measures. Another method of capturing the topological structure of the graph is  
77 presented in [10] and compared in [31]. The curvature on graphs has been studied in many applications  
78 such as finding communities [26], curvature attentive networks [42, 40, 38], over-squashing alleviation  
79 [36], preventing distortion of graph embedding [29], and generating graphs [23]. In previous studies,  
80 the results have shown the existence of a significant relationship between the curvature of the graph  
81 and the informative geometric properties. In this paper, we present that a curvature-based input saving  
82 approach helps to approximate the original graph to a sparse subgraph.

### 83 3 Metric for Combinatorial Subgraphs

84 Let  $\mathcal{G} = (\mathcal{V}, \mathcal{E})$  be a graph with the combinatorial structure of nodes  $\mathcal{V}$  and edges  $\mathcal{E}$ . We can sample  
 85 subgraphs  $\hat{\mathcal{G}} = (\hat{\mathcal{V}}, \hat{\mathcal{E}})$  with sizes  $|\hat{\mathcal{V}}| \ll |\mathcal{V}|$  from  $\mathcal{G}$ . However, numerous subgraphs can be obtained  
 86 from the graph  $\mathcal{G}$ . Therefore, the criteria for determining good subgraphs must be defined according  
 87 to the purpose of sampling. Please note that the subgraphs are sampled to train a large-scale graph  
 88  $\mathcal{G}$  by dividing them into mini-batches  $\{\hat{\mathcal{G}}_i\}$ , because training the large graph at once is difficult.  
 89 Therefore, for unbiased training through mini-batches, the subgraphs should be sampled to be similar  
 90 to the original graph. In graph theory, the traditional metrics for the similarity between two different  
 91 graphs can be defined in various manner.

92 **(Conventional Metric)** The graph edit distance ( $GED$ ) is a measure of matching two different  
 93 graphs by calculating the editing cost to obtain one graph from another, *i.e.*,  $d_{GED}(\mathcal{G}, \hat{\mathcal{G}}) =$   
 94  $\min_{(e_1, e_2, \dots, e_k) \in E(\mathcal{G}, \hat{\mathcal{G}})} \sum_{i=1}^k c(e_i)$ , where  $c(e_i)$  denotes the cost of each edit operation, including  
 95 vertex insertion, vertex deletion, edge insertion, and edge deletion.  $E(\mathcal{G}, \hat{\mathcal{G}})$  denotes the set of edit  
 96 paths. A single path comprises several edit operations  $(e_1, e_2, \dots, e_k)$  used to modify  $\hat{\mathcal{G}}$  to match  
 97 another graph  $\mathcal{G}$ . In contrast to the exact graph matching problem that solves graph isomorphism, the  
 98 graph edit distance measures the similarity between two different graphs (*i.e.*, error-tolerant graph  
 99 matching). Thus, it calculates the minimum error in matching one graph to another. The linear  $p$ -norm  
 100 can also be defined as  $d_A(\mathcal{G}, \hat{\mathcal{G}}) = \|A - \hat{A}\|_p$ , where the  $A$  and  $\hat{A}$  denote the adjacency matrices of  $\mathcal{G}$   
 101 and  $\hat{\mathcal{G}}$ , respectively. However, if the  $GED$  measures the distance  $d_{GED}(\mathcal{G}, \hat{\mathcal{G}})$  between the original  
 102 graph and subgraph, only one edit path is obtained. This is similar to the addition of the cost of  
 103 the number of nodes to the linear distance,  $d_A(\mathcal{G}, \hat{\mathcal{G}})$ . Therefore, the metric  $GED$  and the linear  
 104  $p$ -norm do not reflect the structure of the graph. In contrast, the spectral norm measures the norm  
 105 of the eigenvalues,  $d_\lambda(\mathcal{G}, \hat{\mathcal{G}}) = \sum_{i=1 \dots n} \|\lambda_i - \hat{\lambda}_i\|$ . However, it requires eigendecomposition of the  
 106 original graph and subgraph, the application of which to large graphs is challenging.

107 **(Distributional Metric)** To overcome the problems of conventional metrics, we define the distribu-  
 108 tional metric, *i.e.*, the distance between the probability measures defined on the unweighted graph.  
 109 Let  $(\mathcal{V}, d)$  be a metric space on the connected graph, where  $d(x, y)$  is the distance between the nodes  
 110  $x$  and  $y$ . We define the probability measures for each node to represent the local structure around the  
 111 nodes. Then, the metric  $d_m(\mathcal{G}, \hat{\mathcal{G}})$  between the original graph  $\mathcal{G}$  and the subgraph  $\hat{\mathcal{G}}$  is defined.

112 **Definition 1 (Metric for Deterministic Subgraph)** Let  $\mu$  and  $\hat{\mu}$  be probability measures for original  
 113 and sampled subgraphs, respectively.  $d(x, y)$  is the distance of the geodesic path between nodes  
 114  $x$  and  $y$ , and  $\Pi(\mu, \hat{\mu})$  denotes the set of all couplings between two measures,  $\mu$  and  $\hat{\mu}$ . Then, the  
 115 distance  $d_m(\mathcal{G}, \hat{\mathcal{G}})$  is defined as the distributional distance between  $\mu$  and  $\hat{\mu}$ .

$$d_m(\mathcal{G}, \hat{\mathcal{G}}) = \inf_{\rho \in \Pi(\mu, \hat{\mu})} \int_{x, y \in \mathcal{V} \times \mathcal{V}} d(x, y) \rho(x, y). \quad (1)$$

116 Using Definition 1, we can represent the distance between the original graph and the deterministic  
 117 subgraph. However, because various subgraphs can be obtained from one graph, we extend the metric  
 118 presented in Definition 1 to the metric for non-deterministic subgraphs, as follows:

119 **Definition 2 (Metric for Non-deterministic Subgraph)** A subgraph can be considered as a set of  
 120 sampled nodes and edges derived from combinatorial sampling. Therefore, the distributional metric  
 121 can be redefined as the combination of node-wise metrics or edge-wise metrics. Then, the probability  
 122 measure of the non-deterministic subgraph is represented as the expected value of node-wise measures,  
 123  $\sum_{x \in \mathcal{V}} p(x) \mu_x$ , where  $\mu_x$  is a probability measure for the node  $x$ . Here,  $\mu_x$  can be decomposed as  
 124 edge-wise measures along the edges,  $\sum_{y \in \mathcal{N}(x)} p(y|x) \delta_y$ , where  $p(y|x)$  is the probability that  $y$  is  
 125 sampled to be connected to  $x$ , and  $\delta_y = \mathbf{1}_y$ . We can define the combinatorial metric between the  
 126 original graph and the probabilistic sampled subgraph, as the upper bound of 1.

$$d_m(\mathcal{G}, \hat{\mathcal{G}}) \leq \sum_{x \in \mathcal{V}} p(x) d_m(\mathcal{G}_x, \hat{\mathcal{G}}_x) \leq \sum_{x \in \mathcal{V}} p(x) \left( \sum_{y \in \mathcal{N}(x)} p(y|x) d_m(\mathcal{G}_x, v_y) \right), \quad (2)$$

127 where the metric  $d_m(\mathcal{G}, \hat{\mathcal{G}})$  is upperbounded by the weighted average of the distances between the  
 128 local structural graph  $\mathcal{G}_x$  and each node  $v_y$ . Although the weighted sum of distances for components is  
 129 the upper bound, this method enables the determination of the better subgraph sampling model, using  
 130 only probability models instead of actual subgraph samples. For example, a random edge sampler  
 131 samples the subgraphs with an approximation of  $\sum_{x \in \mathcal{V}} \frac{1}{|\mathcal{V}|} \sum_{y \in \mathcal{N}(x)} \frac{1}{|\mathcal{N}(x)|} d_m(\mathcal{G}_x, v_y)$ , because it is  
 132 a uniform sampling. However, if a sampler has a sampling probability model  $p(x)p(y|x) \propto \frac{1}{d_m(\mathcal{G}_x, v_y)}$   
 133 that is inversely proportional to the distributional difference of each edge, it can be considered a better  
 134 subgraph sampler because it more probable to obtain subgraphs that approximate the original graph.

#### 135 4 Curvature-based Local Structural Approximation

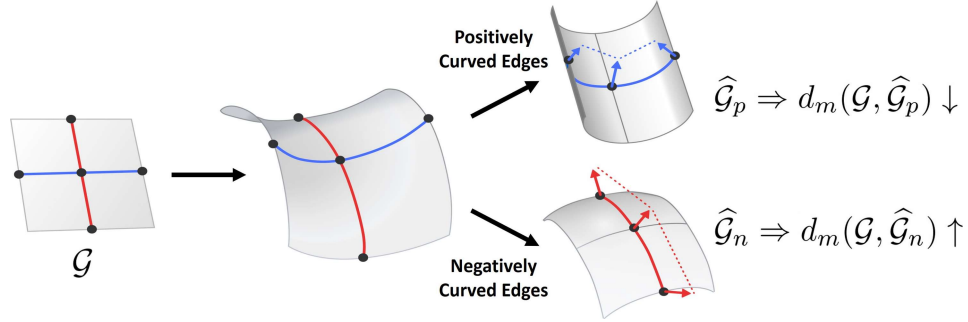


Figure 1: **Curvature-based distributional difference.** If the graph  $\mathcal{G}$  is not in the form of a regular grid, its edges have different distributional distances depending on the structure of the graph. Then, the subgraph  $\hat{\mathcal{G}}_p$  consisting of positively curved edges (blue) are more similar to the original graph than the subgraph  $\hat{\mathcal{G}}_n$  consisting of negatively curved edges (red).

136 We introduce the discrete Ricci curvature  $\kappa_{xy}$  in (4), which is defined as the ratio of the distance  
 137 of probability measures to the distance of nodes. We show that subgraph sampling that maximizes  
 138 the curvature amounts to minimizing the distributional difference between the original graph and  
 139 subgraph. Intuitively,  $d_m$  is determined by the local structure around two nodes, because it can be  
 140 defined as the cost of moving from adjacent nodes of one node to adjacent nodes of another node.  
 141 Thus, subgraph sampling to maximize the curvature enables local structural approximation because it  
 142 minimizes the distribution metric between the original graph and the subgraph.

143 **(Ollivier-Ricci Curvature)** Let  $\mathcal{G} = (\mathcal{V}, \mathcal{E})$  be a graph with nodes  $\mathcal{V}$  and edges  $\mathcal{E}$ .  $\mathcal{N}(x)$  denotes  
 144 adjacent nodes of node  $x \in \mathcal{V}$  and  $d_x$  is the degree of node  $x$ . Assume that  $m_x$  is the probability  
 145 measure of node  $x$  by the random walk kernel  $m$  along the Markov chain. Then, the metric measure  
 146 space can be defined as  $(\mathcal{V}, d, m)$ . The discrete probability measure  $m_x$  for each node  $x \in \mathcal{V}$   
 147 is defined as follows.

$$m_x(v) := \begin{cases} 1_x(v) & \text{if } d_x = 0, \\ \frac{1}{d_x} \cdot \mathbf{1}_{\mathcal{N}(x)}(v) & \text{if } d_x > 0. \end{cases} \quad (3)$$

148 With the probability measures  $m_x, m_y$  for nodes  $x, y \in \mathcal{V}$  of the graph, the transport plan between the  
 149 two probabilities,  $m_x(\mathcal{V})$  and  $m_y(\mathcal{V})$ , is represented as the coupling measure  $\gamma$ , where  $\Pi(m_x, m_y)$   
 150 is the set of measures projecting  $m_x$  to  $m_y$ . Distance  $d(x, y)$  is defined as the length of the shortest path  
 151 between nodes  $x, y$  for the 1-geodesic distance. This is the optimal transport problem between sets  
 152 of nodes  $\mathcal{N}(x)$  and  $\mathcal{N}(y)$ . Then, the 1-Wasserstein distance  $\mathcal{W}_1$  is defined as the minimal cost for  
 153 transportation between two measures, *i.e.*,  $\mathcal{W}_1(m_x, m_y) = \inf_{\gamma \in \Pi(m_x, m_y)} \int_{u, v \in \mathcal{V} \times \mathcal{V}} d(u, v) d\gamma(u, v)$ .

154 If there is at least one path for nodes  $x, y$ , we can define the Ollivier-Ricci curvature  $\kappa_{xy}$  of the edge  
 155  $(x, y)$  in the metric measure space  $(\mathcal{V}, d, m)$ , as follows:

$$\kappa_{xy} = 1 - \frac{\mathcal{W}_1(m_x, m_y)}{d(x, y)}. \quad (4)$$

156 **(Local Structural Approximation)** The Ollivier-Ricci curvature is defined on the metric measure  
 157 space  $(\mathcal{V}, d, m)$  for graphs, in which the large curvature  $\kappa_{xy}$  indicates the small distance  $\mathcal{W}_1(m_x, m_y)$   
 158 between the probability measures  $m_x, m_y$  for two nodes  $x, y$ . Because the probability measure is  
 159 defined through a random-walk kernel, the distribution is distributed uniformly to 1-hop neighbor-  
 160 ing nodes in the unweighted graph. Then it effectively represents the local structural information.  
 161 Therefore, the proposed subgraph sampling proportional to the curvature reduces the distributional  
 162 difference  $d_m(\mathcal{G}_x, \hat{\mathcal{G}}_x)$ , while also approximating the local structure of the graph. As shown in Fig.3,  
 163 even if the same number of edges are sampled equally based on the node, subgraph  $\hat{\mathcal{G}}_p$  with positively  
 164 curved edges can be more distributionally and structurally similar to the original graph than subgraph  
 165  $\hat{\mathcal{G}}_n$  with negatively curved edges.

166 **Proposition 1** Let  $(\mathcal{V}, d, m)$  be the metric space with the random walk  $m$ . Then,  $m_x$  is the probability  
 167 measure defined in 3 for the local structure  $\mathcal{G}_x$ , and  $w_x$  is the probability measure defined as  
 168  $w_x = \sum_{y \in \mathcal{V}} p(y|x) \cdot \delta_y$ , where  $\sum_{y \in \mathcal{N}(x)} p(y|x) = 1$  and  $\delta_y = \mathbf{1}_y$ , for the local structure  $\hat{\mathcal{G}}_x$ . The  
 169 distributional difference of probabilistic sampled subgraphs is bounded by curvatures, as follows:

$$d_m(\mathcal{G}_x, \hat{\mathcal{G}}_x) \leq 2 - \sum_{y \in \mathcal{N}(x)} p(y|x) \kappa_{xy}, \quad (5)$$

170 where  $\kappa_{xy}$  denotes the Ollivier-Ricci curvature of edge  $(x, y)$ . Proposition 1 shows that the distri-  
 171 butional difference around node  $x$  of the probabilistic sampled subgraphs is inversely proportional  
 172 to the expected value of the curvatures of the edges linked to  $x$ . This implies that the distributional  
 173 difference between the sampled subgraph and original graph decreases with the increase in the  
 174 expected value of the curvature; that is, the probability model, which frequently samples edges with  
 175 large curvatures, can obtain more structurally approximated subgraphs. Please note that the upper  
 176 bound of the distributional difference in Proposition 1 can be extended to n-hop to capture a wider  
 177 scope of local structure near the node. Thus, we also present the upper bound of the distributional  
 178 difference between the n-hop diffused probability measure  $m_x^{*n}$  and the probability measure  $w_x$  of  
 179 the probabilistic sampled subgraphs, as follows:

180 **Corollary 1.1**  $m^{*n}$  denotes the probability measure of n-step random walks on a Markov chain. It  
 181 can be considered as the state of n-hop propagation in the original graph. Suppose that the graph  
 182  $\mathcal{G}_p = (\mathcal{V}, \mathcal{E})$  is composed of positively curved edges such as  $\kappa_{xy} \geq \kappa > 0$  for any pair of nodes  $x, y$   
 183 in  $\mathcal{V}$ . Then, the upper bound of distributional difference between  $m_x^{*n}$  and  $w_x$  is bounded as follows.

$$d_m(\mathcal{G}_x^{*n}, \hat{\mathcal{G}}_x) \leq \frac{(1 - \kappa) - (1 - \kappa)^n}{\kappa} + d_m(\mathcal{G}_x, \hat{\mathcal{G}}_x). \quad (6)$$

184 Corollary 1.1 shows that the distributional difference between the n-hop local structure  $\mathcal{G}_x^{*n}$  and  
 185 sampled local structure  $\hat{\mathcal{G}}_x$  is also bounded in relation to the 1-hop local distributional difference in  
 186 Proposition 1. Subsequently, we suggest that subgraphs consisting of edges with large curvatures  
 187 have generalization effects, which can be advantageous for learning the model.

188 **Proposition 2** Let  $\mathcal{P}_i = (x_i = v_0, v_2, \dots, v_n = y_i)$  and  $\mathcal{P}_j = (x_j = u_0, u_1, \dots, u_n = y_j)$  be the  
 189 geodesic paths for any shortest path of  $(x_i, y_i)$  and  $(x_j, y_j)$ , respectively. The distance for each  
 190 edge is defined as  $d(v_i, v_{i+1}) = d(u_i, u_{i+1})$ . Then, if the curvatures of the paths  $\mathcal{P}_i, \mathcal{P}_j$  satisfy the  
 191 inequalities  $\kappa_{v_i v_{i+1}} > \kappa_{u_i u_{i+1}}$  for any edge  $(v_i, v_{i+1})$  and  $(u_i, u_{i+1})$  in the paths, the following  
 192 inequality holds for the gradients between starting and ending nodes in the paths:

$$\nabla_{x_i y_i \in \mathcal{P}_i} (f + \Delta f) \leq \nabla_{x_j y_j \in \mathcal{P}_j} (f + \Delta f) \quad (7)$$

193 for any 1-Lipschitz function  $f$ .

194 Proposition 2 implies that the two paths have the same length but can yield different gradients. The  
 195 gradient is proportional to the sum of the edge curvatures in the path. Therefore, if it is possible to  
 196 walk along the edges with large curvatures, the distance of node features in the starting and ending  
 197 nodes of the path can be close, even for the same length of walks. Thus, propagation by edges with

198 a large curvature can smoothen the feature space. And this can give a generalization effect. The  
 199 locally smoothed feature space can be defined as  $\|f_x - f_y\| < \alpha$  for any pair of nodes  $(x, y)$  with  
 200  $d(x, y) \leq n$ . The small gradient  $\nabla_{xy}$  in the  $n$ -bound indicates that smooth feature space is obtained  
 201 even with relatively distant nodes. In Section 3, we conduct experiments on the generalization effect  
 202 to demonstrate the accuracy with which all nodes can be predicted through learning with only small  
 203 partial nodes.

## 204 5 Localized Curvature-based Combinatorial Sampling

205 Subgraph sampling is used to sample mini-batches for a large-scale graph. However, sampling the  
 206 optimal subgraphs by considering the whole structure of the large graph is challenging. Therefore,  
 207 the previous section shows that local structural approximation of subgraph using curvature is possible  
 208 instead. However, it is still difficult to calculate the exact curvatures of the edges due to the high  
 209 computational cost of solving the optimal transport problem. Thus, we obtain subgraphs through  
 210 combinatorial sampling proportional to the approximated curvatures of the Definition 3 using the  
 211 localized structure of the graph with 3-cycles. We show that the approximated curvatures exhibit  
 212 sufficiently small errors in local structures of sparse graphs.

213 **Definition 3 ([19], Localized Curvature with 3-cycles)**  $d_x$  and  $d_y$  denote the degree of nodes  $x$  and  
 214  $y$ , respectively.  $\Delta_{\sharp}(x, y)$  represents the number of triangles (3-cycles) including the edge  $(x, y)$ . The  
 215 operations  $d_x \wedge d_y$  and  $d_x \vee d_y$  denote  $\min[d_x, d_y]$  and  $\max[d_x, d_y]$ , respectively.  $(\cdot)_+$  is defined  
 216 as  $\max[\cdot, 0]$ . Then, the localized curvature  $\kappa_{xy}$  for the edge  $(x, y)$  has the following lower bound.

$$\kappa_{xy} \geq - \left( 1 - \frac{1}{d_x} - \frac{1}{d_y} - \frac{\Delta_{\sharp}(x, y)}{d_x \wedge d_y} \right)_+ - \left( 1 - \frac{1}{d_x} - \frac{1}{d_y} - \frac{\Delta_{\sharp}(x, y)}{d_x \vee d_y} \right)_+ + \frac{\Delta_{\sharp}(x, y)}{d_x \vee d_y}. \quad (8)$$

217 The lower bound of  $\kappa_{xy}$  in (8) can  
 218 be considered the localized curvature  
 219 for ((4) and Fig.2A) in the 1-hop local  
 220 structures  $\mathcal{N}(x) \cup \mathcal{N}(y)$ . As this local-  
 221 ized curvature only considers adjacent  
 222 neighbors, it is not accurate. However,  
 223 the localized curvature with 3-cycles  
 224 ((8) and Fig.2B) is within the tolerance range of the exact curvature for sparse graphs. We also present  
 225 that other conventional subgraph sampling methods are related to more approximated curvatures  
 226 with no cycles ((9) and Fig.2C), and argue that curvature is closely related to subgraph sampling.  
 227 It assumes that there are no cycle  $\Delta_{\sharp}(x, y) = 0$  in the local structure of the graph even if there are  
 228 cycles. Therefore, the lower bound of the curvature without cycles [24] is defined as follows.

$$\kappa_{xy} \geq -2 \left( 1 - \frac{1}{d_x} - \frac{1}{d_y} \right)_+, \quad (9)$$

229 where  $d_x$  and  $d_y$  denote the degrees of nodes  $x, y$  of edge  $(x, y)$ , respectively. Conventional combina-  
 230 torial subgraph sampling methods are related to this localized curvature without a cycle, as Table 1.

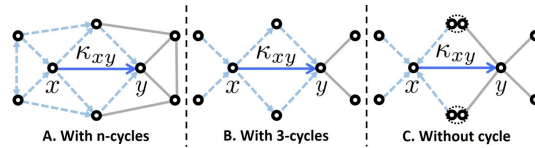


Figure 2: Approximated curvatures in the local structure.

Table 1: Conventional methods can be interpreted as sampling related to the coarse curvature.

Sampler	Probability model	With curvature
Edge[45]	$p(e_{xy}) \propto \frac{1}{d_x} + \frac{1}{d_y}$	$p(e_{xy}) \propto \frac{\kappa_{xy} + 2}{2}$
Node[45]	$p(x) \propto (\sum_{y \sim x} \frac{1}{d_x} + \frac{1}{d_y} - 1)^2$	$p(x) \propto (\sum_{y \sim x} \frac{\kappa_{xy} + 2}{2} - 1)^2$
Cluster[7]	$p(x) \propto c(x)$	$p(x) \propto \frac{\sum_{y \sim x} (\kappa_{xy} + 2) - 4}{3d - 1}$

232 We show that the local structure  $\mathcal{N}(x) \cup \mathcal{N}(y)$  of the graph does not have the shortest path beyond  
 233 5-cycles, thus the localized curvature with 3-cycles has very small errors in the sparse large graph.

234 **Proposition 3 (Error bound of localized curvature)** Let  $\mathcal{G}(n, p)$  be the ER-graph (Erdős-Rényi  
 235 model) with  $n > 4$  nodes and edges connected by the probability  $0 \leq p \leq 1$ . Then, the degrees  $d_x, d_y$   
 236 of nodes  $x, y$  are expected as  $d_x = d_y = d = (n - 1)p$ . Let  $\Delta_{\sharp}(x, y)$  be the number of 3-cycles,  
 237  $\square_{\sharp}(x, y)$  be the number of 4-cycles,  $\diamond_{\sharp}(x, y)$  be the number of 5-cycles. In the local structure, the  
 238 shortest distance between nodes can be obtained by considering only 5-cycles or less, so there is a  
 239 small error in the approximated curvature  $\hat{\kappa}_{xy}$  with 3-cycles for sparse large graphs:

$$\|\kappa_{xy} - \hat{\kappa}_{xy}\| \leq \frac{2}{d}\square_{\sharp}(x, y) + \frac{1}{d}\diamond_{\sharp}(x, y) \leq 2dp + 2d^2p \quad (10)$$

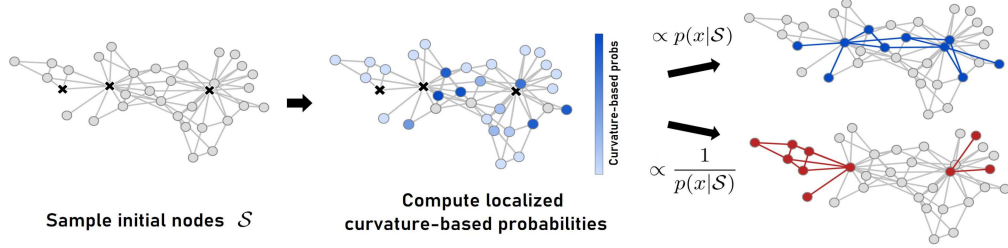


Figure 3: **Curvature-based subgraph sampling.** First, we sample the initial nodes  $\mathcal{S}$ , then the probabilities  $p(x|\mathcal{S})$  is computed based on the curvatures. With the proposed method, we can sample nodes (blue) to maximize the curvatures in a subgraph.

240 **(Proposed Method)** We propose a localized curvature-based sampling method to sample the sub-  
 241 graphs from large graphs. There are studies [8, 30, 34, 2] that solve optimization problems to sample  
 242 the subgraphs. However, because they have difficulty in dealing with large graphs, we present a  
 243 combinatorial approach that samples nodes and edges as like [14, 45, 7, 1]. Furthermore, while  
 244 conventional methods have been described through variance reduction or node degree, we show  
 245 that they can be interpreted by using the coarse curvature (9) in Table 1. Therefore, we propose  
 246 the algorithm that locally approximates the optimal subgraph by finding the subgraph with large  
 247 curvatures in Definition 3.

248 The curvature  $\kappa_{xy}$  is defined for edges  $(x, y)$ , in which the sampling probability for each edge is  
 249 defined as  $p(y|x) \propto \kappa_{xy}$  in Definition 2. However, because  $p(y|x)$  is bounded in the local structure, it  
 250 can be defined via normalization, *i.e.*,  $p(y|x) = \frac{\kappa_{xy}}{\sum_{v \in \mathcal{N}(x)} \kappa_{xv}}$ . Alternatively, the probability for each  
 251 edge can be defined directly to the structural normalized curvature, *i.e.*,  $p(y|x) \propto \frac{\kappa_{xy}}{d_y}$ .

252 Using the above probability model, we extend local optimal subgraphs instead of finding a global  
 253 optimal subgraph. In the beginning, there are no sampled node, so initial nodes  $x_0 \in \mathcal{S}_0$  are sampled  
 254 by  $p(x_0|\mathcal{V}) \propto \sum_{y \in \mathcal{N}(x_0), y \in \mathcal{V}} p(x_0|y)$ . After sampling the initial nodes, linked nodes  $x_{i+1} \in \mathcal{N}(\mathcal{S}_i)$   
 255 have sampling probabilities  $p(x_{i+1}|\mathcal{S}_i) \propto \sum_{y \in \mathcal{N}(x_{i+1}), y \in \mathcal{S}_i} p(x_{i+1}|y)$ . Our method starts at the  
 256 initial nodes  $\mathcal{S}_0$ , then extends to the connected nodes  $\mathcal{S}_1$  to maximize the sum of curvatures of edges  
 257 in the subgraph  $\hat{\mathcal{G}} = \mathcal{S}_0 \cup \mathcal{S}_1 \cup \dots \cup \mathcal{S}_t$ . If we sample  $n$  subgraphs with the size of  $m$  in  $t$  steps, the  
 258 whole pipeline of the proposed method is in Algorithm 1. Further details can be found in Appendix E.

---

**Algorithm 1** Localized Curvature-Based Sampling (LoCur)

---

**Inputs:**  $\mathcal{G} = (\mathcal{V}, \mathcal{E})$ , iters  $n$ , sample size  $m$ , steps  $t$  / **Output:** sampled subgraphs  $\{\hat{\mathcal{G}}_i\}_{i=1}^n$

$p(x|\mathcal{V}) \propto \sum_{y \sim x, y \in \mathcal{V}} p(x|y)$  ▷ compute localized curvature-based probabilities

**for**  $k = 1$  **to**  $n$  **do**

$\mathcal{S}_0 = \{v_0, v_1, \dots, v_{\lfloor m/s \rfloor}\} \sim p(x|\mathcal{V})$  ▷ sample initial nodes

**for**  $i = 0$  **to**  $t - 1$  **do**

$p(x|\mathcal{S}_i) \propto \sum_{y \in \mathcal{N}(x), y \in \mathcal{S}_i} p(x|y)$  ▷ compute localized curvature-based probabilities

$\mathcal{S}_{i+1} = \mathcal{S}_i \cup \{u_0, u_1, \dots, u_{\lfloor m/s \rfloor}\} \sim p(x|\mathcal{S}_i)$  ▷ sample extended nodes

**end for**

$\hat{\mathcal{G}}_k = \mathcal{S}_t$

**end for**

---

## 259 6 Experiments

260 Our method proposes to sample the subgraphs that maximize the curvature more directly compared to  
 261 conventional methods. Therefore, although our method cannot calculate the exact Ollivier-Ricci  
 262 curvature for the large-scale graphs, it can present the exact curvature calculated by [27] for small  
 263 graphs (Cora graph [25] with 2708 nodes and 5429 edges, Citeseer graph [12] with 3312 nodes  
 264 and 4732 edges, and the Pubmed graph [32] with 19717 nodes and 44338 edges). The following  
 265 experiment in Table 2 was evaluated for 1000 subgraphs with about 10% (200/2708, 300/3327,  
 2000/19717) partial nodes.

Table 2: Comparison of Ollivier-Ricci curvature using the Cora, Citeseer, Pubmed graphs.

Ollivier-Ricci Curvature	random	neighbor	node	edge	random walk	multi clusters	PPR	LoCur (Ours)	original graph
Cora	-0.08	-0.06	-0.09	-0.08	-0.07	-0.02	-0.08	<b>+0.00</b>	-0.07
Citeseer	-0.05	-0.06	-0.09	-0.06	-0.06	-0.01	-0.07	<b>+0.02</b>	-0.06
Pubmed	-0.08	-0.07	<b>-0.05</b>	-0.07	-0.07	-0.07	-0.08	<b>-0.05</b>	-0.08

266

267 We also show sampled subgraphs for the karate club graph [44] with 34 nodes and 78 edges, which is  
 268 a very small graph, and present results for one of the REDDIT-BINARY graphs [13] with 400 nodes  
 269 and 460 edges. With this experiment, we can examine the structure sampled by the subgraph. As  
 270 shown in Fig.4, our method samples the subgraphs to include representative structures without bias  
 271 compared to other methods.

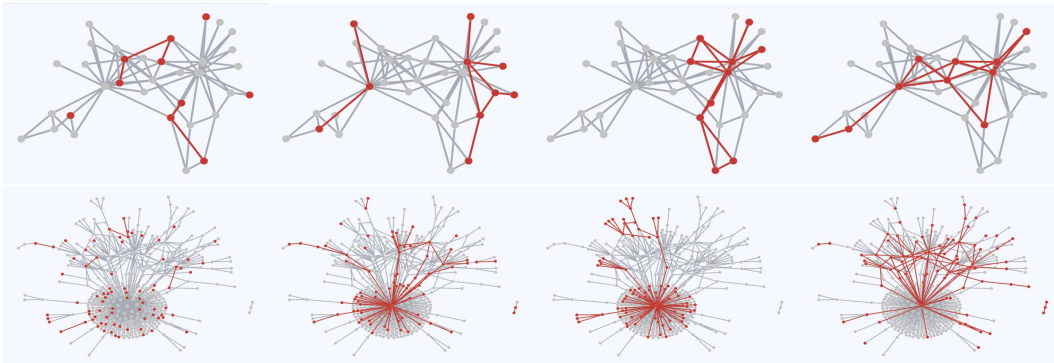


Figure 4: **Subgraph examples for Karate club and REDDIT-BINARY graphs.** This figure show the subgraphs of random, edge, cluster, and LoCur(ours) sampling from left to right. Additional results can be found in Appendix F.

272 These sampled subgraphs are typically evaluated by the tasks such as node classification and graph  
 273 classification. However, in the case of semi-supervised node classification, evaluation can be af-  
 274 fected by train, valid, and test ratios of nodes within sampled subgraphs. Therefore, we present a  
 275 labeling task that evaluates the entire nodes (100%) by learning only one sampled subgraph of the  
 276 specific proportions (1%, 5%, 10%) in 100 experiments. Table 3 shows that our method induces the  
 277 generalization effect, which yields good performance even with very few nodes.

278 Our subgraph sampling method can train large-scale graphs, such as mini-batch training, by sampling  
 279 approximated subgraphs, which are used only for training and the entire graph is used for evaluation.  
 280 Because each graph has a different size, the size of subgraphs are different for each graph. In addition,  
 281 all experiments can be reproduced using a common random seed. The sampling costs are negligible  
 282 because the subgraphs are shuffled and reused to configure the batches following the initial sampling.  
 283 The proposed method was evaluated based on the highest valid accuracy without any methods, such  
 284 as early stop or regularization. Consequently, the average accuracy and standard deviation of the  
 285 training results were obtained for 100 subgraphs by performing the experiment 10 times.



Table 3: Comparison of labeling task using the ogbn-arxiv, ogbn-mag graphs.

Labeling	arxiv-1 (%)	arxiv-5 (%)	arxiv-10 (%)	mag-1 (%)	mag-5 (%)	mag-10 (%)
random	57.02±2.55	65.78±0.71	68.16±0.31	<u>25.93±0.49</u>	29.25±0.21	30.94±0.15
neighbor	58.13±1.37	66.28±0.44	68.73±0.30	24.95±0.45	30.42±0.18	<u>32.66±0.13</u>
node	58.55±1.35	<u>67.12±0.39</u>	<u>69.51±0.23</u>	25.03±0.45	30.42±0.16	32.30±0.11
edge	<u>60.42±0.88</u>	67.10±0.33	69.31±0.22	25.67±0.41	<u>30.55±0.18</u>	32.47±0.13
random walk	59.37±0.84	66.66±0.33	68.90±0.23	25.49±0.35	30.47±0.16	32.46±0.13
cluster	53.09±1.80	64.54±0.54	67.63±0.33	22.03±0.65	29.14±0.22	31.78±0.19
ppr	56.74±3.46	66.13±0.78	68.35±0.43	<b>26.06±0.36</b>	30.41±0.20	32.54±0.14
LoCur (Ours)	<b>62.01±0.72</b>	<b>68.09±0.29</b>	<b>70.14±0.19</b>	25.69±0.48	<b>30.78±0.22</b>	<b>32.86±0.15</b>

286 The ogbn-arxiv graph [16] in Table 4 comprises 169,343 nodes and 1,166,243 edges, which is a  
 287 directed graph representing citations. We trained the graph neural models with undirected normaliza-  
 288 tion and sampled 100 subgraphs with the size of 1,700(1%) to construct mini-batches. Because our  
 289 sampling method uses only the structural information of the graph, it does not directly improve the  
 290 accuracy of the node classification task. Nevertheless, our method produced competitive results.

291 The ogbn-mag graph [16] in Table 4 consists of 736,389 nodes and 10,792,672 edges. We sampled  
 292 100 subgraphs with the size of 7,000(1%) to construct mini-batches, and performed the mini-batch  
 293 training using the sampled subgraphs. The evaluation of the compared methods was conducted using  
 294 the entire graph. In the case of the GCNII method and ogbn-mag dataset, inferring the original graph  
 295 is difficult; thus, the results are not available. The accuracy of the sampling methods depends on  
 296 the characteristics of the graph because subgraph sampling methods use only the graph structural  
 297 information without feature information. In the case of the ogbn-mag graph, aggregating the feature  
 298 points of nearby nodes, for example, clustering, induced good results.

299 Tables 3 and 4, and additional results <sup>1</sup> show that the proposed method produced competitive results  
 300 for various graphs and GNNs. Our method can efficiently train GNNs using only subgraphs with  
 301 partial nodes (1%) compared to the GNNs trained for the entire graph.

Table 4: Comparison of node classification using the ogbn-arxiv and ogbn-mag graphs.

Node	arxiv/GCN		arxiv/GraphSAGE		mag/GCN		mag/GraphSAGE	
	Valid acc (%)	Test acc (%)	Valid acc (%)	Test acc (%)	Valid acc (%)	Test acc (%)	Valid acc (%)	Test acc (%)
random	65.60±1.21	64.43±2.06	67.15±0.35	66.54±0.63	28.79±0.80	30.02±0.98	30.89±0.53	31.87±0.47
neighbor	70.49±0.22	69.00±0.59	<u>71.12±0.16</u>	<u>70.11±0.23</u>	32.60±0.62	33.14±0.80	32.83±0.30	33.64±0.37
node	68.44±0.24	67.56±0.37	65.32±0.15	64.20±0.25	28.15±0.42	29.35±0.49	26.72±0.53	28.06±0.57
edge	69.97±0.27	69.12±0.61	70.53±0.19	69.23±0.30	30.83±0.46	31.41±0.46	31.70±0.32	32.66±0.41
random walk	70.39±0.19	<u>69.41±0.29</u>	70.78±0.17	69.55±0.26	31.86±0.18	32.48±0.29	32.08±0.47	32.89±0.48
cluster	<u>70.58±0.35</u>	69.35±0.62	70.56±0.19	69.09±0.39	<u>33.93±0.37</u>	<u>34.82±0.39</u>	<u>34.41±0.48</u>	<u>35.09±0.51</u>
ppr	67.70±0.55	66.45±0.83	71.10±0.23	70.04±0.62	29.67±0.57	30.85±0.68	31.31±0.52	32.04±0.63
LoCur (Ours)	<b>70.91±0.24</b>	<b>69.53±0.57</b>	<b>71.29±0.15</b>	<b>70.15±0.31</b>	<b>34.54±0.64</b>	<b>35.08±0.77</b>	<b>34.69±0.65</b>	<b>35.32±0.86</b>
original graph	73.15±0.08	71.97±0.32	73.08±0.21	71.65±0.46	36.54±0.18	36.74±0.26	36.55±0.40	36.69±0.35

## 302 7 Conclusion

303 To learn a large graph by dividing it into subgraphs, the subgraphs should be sampled to represent the  
 304 original graph. While finding substructures using curvature in large graphs has been widely studied,  
 305 we propose that the coarse Ollivier-Ricci curvature bounded by the local structure is closely related  
 306 to conventional combinatorial subgraph sampling methods. Therefore, our method performs a local  
 307 optimization search to maximize the curvature of the subgraph based on the localized curvature.  
 308 Consequently, our method can obtain the combinatorial subgraphs to approximate the original graph  
 309 by the distribution metric. The experimental results show that subgraphs with the edges of large  
 310 curvature are suitable for representing the original graph.

<sup>1</sup>Please refer to Appendix F for additional experiments.

311 **References**

- 312 [1] Aleksandar Bojchevski, Johannes Klicpera, Bryan Perozzi, Amol Kapoor, Martin Blais, Benedek  
313 Rózemberczki, Michal Lukasik, and Stephan Günnemann. Scaling graph neural networks with approximate  
314 pagerank. In *ACM SIGKDD*, 2020.
- 315 [2] Francesco Bonchi, David García-Soriano, Atsushi Miyauchi, and Charalampos E Tsourakakis. Finding  
316 densest k-connected subgraphs. *Discrete Applied Mathematics*, 305:34–47, 2021.
- 317 [3] Chen Cai, Dingkang Wang, and Yusu Wang. Graph coarsening with neural networks. In *ICLR*, 2021.
- 318 [4] Jianfei Chen, Jun Zhu, and Le Song. Stochastic training of graph convolutional networks with variance  
319 reduction. *arXiv preprint arXiv:1710.10568*, 2017.
- 320 [5] Jie Chen, Tengfei Ma, and Cao Xiao. Fastgen: fast learning with graph convolutional networks via  
321 importance sampling. *arXiv preprint arXiv:1801.10247*, 2018.
- 322 [6] Ming Chen, Zhewei Wei, Zengfeng Huang, Bolin Ding, and Yaliang Li. Simple and deep graph convolu-  
323 tional networks. In *ICML*, 2020.
- 324 [7] Wei-Lin Chiang, Xuanqing Liu, Si Si, Yang Li, Samy Bengio, and Cho-Jui Hsieh. Cluster-gen: An efficient  
325 algorithm for training deep and large graph convolutional networks. In *ACM SIGKDD*, 2019.
- 326 [8] Alessio Conte, Andrea Marino, Roberto Grossi, Takeaki Uno, and Luca Versari. Proximity search for  
327 maximal subgraph enumeration. *arXiv preprint arXiv:1912.13446*, 2019.
- 328 [9] Michaël Defferrard, Xavier Bresson, and Pierre Vandergheynst. Convolutional neural networks on graphs  
329 with fast localized spectral filtering. *NIPS*, 2016.
- 330 [10] Robin Forman. Bochner’s method for cell complexes and combinatorial ricci curvature. *Discrete and  
331 Computational Geometry*, 29(3):323–374, 2003.
- 332 [11] Fabrizio Frasca, Emanuele Rossi, Davide Eynard, Ben Chamberlain, Michael Bronstein, and Federico  
333 Monti. Sign: Scalable inception graph neural networks. *arXiv preprint arXiv:2004.11198*, 2020.
- 334 [12] C Lee Giles, Kurt D Bollacker, and Steve Lawrence. Citeseer: An automatic citation indexing system. In  
335 *Proceedings of the third ACM conference on Digital libraries*, pages 89–98, 1998.
- 336 [13] Will Hamilton, Zhitao Ying, and Jure Leskovec. Inductive representation learning on large graphs. *Advances  
337 in neural information processing systems*, 30, 2017.
- 338 [14] William L Hamilton, Rex Ying, and Jure Leskovec. Inductive representation learning on large graphs. In  
339 *NIPS*, 2017.
- 340 [15] Arman Hasanzadeh, Ehsan Hajiramezani, Shahin Boluki, Mingyuan Zhou, Nick Duffield, Krishna  
341 Narayanan, and Xiaoning Qian. Bayesian graph neural networks with adaptive connection sampling. In  
342 *ICML*, 2020.
- 343 [16] Weihua Hu, Matthias Fey, Marinka Zitnik, Yuxiao Dong, Hongyu Ren, Bowen Liu, Michele Catasta,  
344 and Jure Leskovec. Open graph benchmark: Datasets for machine learning on graphs. *arXiv preprint  
345 arXiv:2005.00687*, 2020.
- 346 [17] Wenbing Huang, Tong Zhang, Yu Rong, and Junzhou Huang. Adaptive sampling towards fast graph  
347 representation learning. *arXiv preprint arXiv:1809.05343*, 2018.
- 348 [18] Yu Jin, Andreas Loukas, and Joseph JaJa. Graph coarsening with preserved spectral properties. In *AISTATS*,  
349 2020.
- 350 [19] Jürgen Jost and Shiping Liu. Ollivier’s ricci curvature, local clustering and curvature-dimension inequalities  
351 on graphs. *Discrete & Computational Geometry*, 51(2):300–322, 2014.
- 352 [20] Thomas N Kipf and Max Welling. Semi-supervised classification with graph convolutional networks.  
353 *arXiv preprint arXiv:1609.02907*, 2016.
- 354 [21] Johannes Klicpera, Aleksandar Bojchevski, and Stephan Günnemann. Predict then propagate: Graph neural  
355 networks meet personalized pagerank. *arXiv preprint arXiv:1810.05997*, 2018.
- 356 [22] Johannes Klicpera, Stefan Weissenberger, and Stephan Günnemann. Diffusion improves graph learning. In  
357 *NeurIPS*, 2019.

- 358 [23] Jianxin Li, Xingcheng Fu, Qingyun Sun, Cheng Ji, Jiajun Tan, Jia Wu, and Hao Peng. Curvature graph  
359 generative adversarial networks. In *WWW*, 2022.
- 360 [24] Yong Lin and Shing-Tung Yau. Ricci curvature and eigenvalue estimate on locally finite graphs. *Mathe-*  
361 *matical research letters, ISSN 1073-2780, Vol. 17, N° 2-3, 2010, pages. 343-356*, 17, 03 2010.
- 362 [25] Andrew Kachites McCallum, Kamal Nigam, Jason Rennie, and Kristie Seymore. Automating the construc-  
363 tion of internet portals with machine learning. *Information Retrieval*, 3(2):127–163, 2000.
- 364 [26] Chien-Chun Ni, Yu-Yao Lin, Feng Luo, and Jie Gao. Community detection on networks with ricci flow.  
365 *Scientific reports*, 9(1):1–12, 2019.
- 366 [27] Chien-Chun Ni, Yu-Yao Lin, Feng Luo, and Jie Gao. Community detection on networks with ricci flow.  
367 *Scientific reports*, 9(1):1–12, 2019.
- 368 [28] Yann Ollivier. Ricci curvature of markov chains on metric spaces. *Journal of Functional Analysis*,  
369 256(3):810–864, 2009.
- 370 [29] Hongbin Pei, Bingzhe Wei, Kevin Chen-Chuan Chang, Chunxu Zhang, and Bo Yang. Curvature regular-  
371 ization to prevent distortion in graph embedding. *arXiv preprint arXiv:2011.14211*, 2020.
- 372 [30] Daniel Rehfeldt, Henriette Franz, and Thorsten Koch. Optimal connected subgraphs: Formulations and  
373 algorithms. 2020.
- 374 [31] Areejit Samal, RP Sreejith, Jiao Gu, Shiping Liu, Emil Saucan, and Jürgen Jost. Comparative analysis of  
375 two discretizations of ricci curvature for complex networks. *Scientific reports*, 8(1):1–16, 2018.
- 376 [32] Prithviraj Sen, Galileo Namata, Mustafa Bilgic, Lise Getoor, Brian Gallagher, and Tina Eliassi-Rad.  
377 Collective classification in network data. *AI magazine*, 29(3):93–93, 2008.
- 378 [33] Ming Shao, Xindong Wu, and Yun Fu. Scalable nearest neighbor sparse graph approximation by exploiting  
379 graph structure. *IEEE transactions on big data*, 2(4):365–380, 2016.
- 380 [34] Renata Sotirov. On solving the densest k-subgraph problem on large graphs. *Optimization Methods and*  
381 *Software*, 35(6):1160–1178, 2020.
- 382 [35] Chuxiong Sun and Guoshi Wu. Adaptive graph diffusion networks with hop-wise attention. *arXiv preprint*  
383 *arXiv:2012.15024*, 2020.
- 384 [36] Jake Topping, Francesco Di Giovanni, Benjamin Paul Chamberlain, Xiaowen Dong, and Michael M.  
385 Bronstein. Understanding over-squashing and bottlenecks on graphs via curvature. In *ICLR*, 2022.
- 386 [37] Petar Veličković, Guillem Cucurull, Arantxa Casanova, Adriana Romero, Pietro Liò, and Yoshua Bengio.  
387 Graph attention networks. In *ICLR*, 2018.
- 388 [38] Jinhuan Wang, Pengtao Chen, Bin Ma, Jiajun Zhou, Zhongyuan Ruan, Guanrong Chen, and Qi Xuan.  
389 Sampling subgraph network with application to graph classification. *IEEE Transactions on Network*  
390 *Science and Engineering*, 8(4):3478–3490, 2021.
- 391 [39] Felix Wu, Amauri Souza, Tianyi Zhang, Christopher Fifty, Tao Yu, and Kilian Weinberger. Simplifying  
392 graph convolutional networks. In *ICML*, 2019.
- 393 [40] Wei Wu, Guangmin Hu, and Fucai Yu. Ricci curvature-based semi-supervised learning on an attributed  
394 network. *Entropy*, 23(3):292, 2021.
- 395 [41] Keyulu Xu, Chengtao Li, Yonglong Tian, Tomohiro Sonobe, Ken-ichi Kawarabayashi, and Stefanie Jegelka.  
396 Representation learning on graphs with jumping knowledge networks. In *ICML*, 2018.
- 397 [42] Ze Ye, Kin Sum Liu, Tengfei Ma, Jie Gao, and Chao Chen. Curvature graph network. In *ICLR*, 2020.
- 398 [43] Jaemin Yoo, U Kang, Mauro Scanagatta, Giorgio Corani, and Marco Zaffalon. Sampling subgraphs with  
399 guaranteed treewidth for accurate and efficient graphical inference. In *WSDM*, 2020.
- 400 [44] Wayne W Zachary. An information flow model for conflict and fission in small groups. *Journal of*  
401 *anthropological research*, 33(4):452–473, 1977.
- 402 [45] Hanqing Zeng, Hongkuan Zhou, Ajitesh Srivastava, Rajgopal Kannan, and Viktor Prasanna. Graphsaint:  
403 Graph sampling based inductive learning method. *arXiv preprint arXiv:1907.04931*, 2019.

404 **Checklist**

- 405 1. For all authors...
- 406 (a) Do the main claims made in the abstract and introduction accurately reflect the paper’s  
407 contributions and scope? [Yes]
- 408 (b) Did you describe the limitations of your work? [Yes]  
409 → In Section 5, *our method focuses on finding the optimal subgraphs by combining*  
410 *local optimal structures instead of global optimal structures. Because the exact Ollivier-*  
411 *Ricci curvature is difficult to calculate, we propose a probability model proportional to*  
412 *the locally approximated curvature.*
- 413 (c) Did you discuss any potential negative societal impacts of your work? [N/A]
- 414 (d) Have you read the ethics review guidelines and ensured that your paper conforms to  
415 them? [N/A]
- 416 2. If you are including theoretical results...
- 417 (a) Did you state the full set of assumptions of all theoretical results? [Yes]  
418 → *We presented the theoretical assumptions for (Definitions 1 and 2; Proposition 1, 2,*  
419 *and 3; Corollary 1.1; and Table 1).*
- 420 (b) Did you include complete proofs of all theoretical results? [Yes]  
421 → *We proved the theoretical results in Appendix D.*
- 422 3. If you ran experiments...
- 423 (a) Did you include the code, data, and instructions needed to reproduce the main experi-  
424 mental results (either in the supplemental material or as a URL)? [No]
- 425 (b) Did you specify all the training details (e.g., data splits, hyperparameters, how they  
426 were chosen)? [Yes]  
427 → *We explained the experimental details in Appendix F.*
- 428 (c) Did you report error bars (e.g., with respect to the random seed after running experi-  
429 ments multiple times)? [Yes]  
430 → *We conducted the experiments (Tables 2,3, and 4) using a fixed common random*  
431 *seed, and also presented mean and standard deviation for many samples (100~1000).*
- 432 (d) Did you include the total amount of compute and the type of resources used (e.g., type  
433 of GPUs, internal cluster, or cloud provider)? [Yes]  
434 → *Environmental settings for the experiments were also presented in Appendix F.*
- 435 4. If you are using existing assets (e.g., code, data, models) or curating/releasing new assets...
- 436 (a) If your work uses existing assets, did you cite the creators? [Yes]  
437 → *We used those in [27] to compute the exact Ollivier-Ricci curvatures in Table 2. We*  
438 *evaluated sampling methods using benchmark graphs in [16].*
- 439 (b) Did you mention the license of the assets? [N/A]
- 440 (c) Did you include any new assets either in the supplemental material or as a URL? [N/A]  
441
- 442 (d) Did you discuss whether and how consent was obtained from people whose data you’re  
443 using/curating? [N/A]
- 444 (e) Did you discuss whether the data you are using/curating contains personally identifiable  
445 information or offensive content? [N/A]
- 446 5. If you used crowdsourcing or conducted research with human subjects...
- 447 (a) Did you include the full text of instructions given to participants and screenshots, if  
448 applicable? [N/A]
- 449 (b) Did you describe any potential participant risks, with links to Institutional Review  
450 Board (IRB) approvals, if applicable? [N/A]
- 451 (c) Did you include the estimated hourly wage paid to participants and the total amount  
452 spent on participant compensation? [N/A]